Int. J. Appl. Comput. Math (2017) 3:1077–1101
DOI 10.1007/s40819-016-0163-x

ORIGINAL PAPER

# Simulation of Tumor Response to Immunotherapy Using a Hybrid Cellular Automata Model

**Samira Zouhri**[1] · **Smahane Saadi**[1] · **Mostafa Rachik**[1]

Published online: 29 March 2016


**Abstract** A cellular automata model is presented to describe the interaction between a growing tumor next to the presence of nutrient elements, and the immune response as well as the immunotherapy intervention and its stimulator effect on immune cell activity. A comparison between tumor growth before and after immunotherapy effect is discussed, and many characteristics of simulated tumor growth patterns are extracted such as the fractal dimension, the fractality of tumor boundary and the number of cancerous cells on tumor periphery. The simulation results shed light on the factor that may play a central role in immunotherapy effectiveness and which is related to tumor morphology.

**Keywords** Hybrid cellular automata · Immunotherapy · Interleukin-2 · Tumor morphology · CTL induction

## Introduction

Cancer is still a main cause of death in the world, with approximately 14 million new cases and 8.2 million cancer related deaths in 2012 (World cancer report 2014). Several scientific investigations have been done or are in progress to understand the biological mechanisms of cancer establishment and destruction in order to prevent and manage the disease by exploring new treatment techniques. In the past few years, there has been a major breakthrough concerning new treatments for cancer. One of the most important ones is immunotherapy. The basic idea behind immunotherapy is to stimulate the immune system and increase its effectiveness at eliminating cancer cells on its own.

Mathematical models are tools that help to understand the complexity of cancer growth, the cell interaction as well as the therapeutic intervention and its effect on tumor development

✉ Samira Zouhri
samira_zouhri@hotmail.com

[1] Department of Mathematics and Computer Sciences, Faculty of Sciences Ben M'Sik-Casablanca, Hassan II University, Casablanca, Avenue Commandant Driss ELHARTI, B.P. 7955, 20800 Casablanca, Morocco

[4,7,15–17,25,32,33,45]. Two approaches have been used to describe the tumor growth: the continuous models [1,21], and the discrete models [2,22,24,36,41,42,52] which may use the cellular automata methods.

Cellular automata (CA) are mathematical models of systems where time, space and state are discrete and each cell changes its state according to its current state, the state of nearest neighbors and local rules. A number of characteristics make the CA models attractive for simulating and studying tumor growth, such as the use of microscopic-scale in CA rules for each time step, which help to understand the phenomena at a microscopic level, cell's level.

Ferreira et al. [17] proposed a reaction–diffusion model for avascular tumor growth, including the cell proliferation, motility and death as well as the competition between tumor and normal cells for nutrients. Their results indicate that the tumor morphology may be affected by the competition for nutrients among normal and cancer cells. What was not considered in their model is the immune response intervention, which have lead [32] to develop a new model where they have investigated the dynamics of tumor–immune system interactions by including the natural killer cells and cytotoxic T lymphocytes and using a hybrid cellular automata—a deterministic PDE, they have taken into account the immune cell migration and death as well as the tumor lysis due to the immune cells. They found that depending on the strength of T cell recruitment and T cell death parameters, tumor grew with stable or unstable oscillations and in some cases tumor was eradicated completely.

The major intention of this work is to further develop the CA model of [32] by including more biological implementations of the immunotherapy intervention. Particularly, we consider the effects of interleukin-2 on the immune response, the cytokine that plays a central role in the activation and proliferation of immune cells, which make us able to describe the interaction of tumor and immune cells after and before therapy intervention, to study the effect of treatment on this interaction and to understand other factor that may affect the therapy effectiveness.

The paper is organized as follows: in "CA Model" section we present a biological background of tumor and immune cells as well as the immunotherapy intervention, and the CA method. In "Simulation and Results Without Immunotherapy Intervention" section, simulation and results without immunotherapy intervention are developed. Then, in "Tumor Characteristics Obtained from the Growth Patterns" section, we discuss the tumor characteristics obtained from the growth patterns. Finally, in "Simulation and Results with Immunotherapy Intervention" section, simulation and results for the immunotherapy intervention are presented.

## CA Model

### Biological Background

In normal cellular tissue there is a constant balance between proliferation and cell death. The cells are born, complete their mission and start off their self destruction (apoptosis). The immune system monitors the body with an innate or natural defense mechanism, it recruits a coordinated set of innate immune cells including Natural Killer cells (NK). NK cells represent the first line of defense against infected or cancerous cells, their action is determined via activating and inhibitory receptors presented on their surface. NK cells intervene to protect the body with a quick and immediate immune response, traveling through the blood stream and the lymph system to the extracellular fluid, where they find and kill foreign cells [6]. NK

cells don't recognize in advance the target cell, their mode of action is the same whatever the infectious agent met.

In the case of cancer, cells are born, do their task, and refuse apoptosis. Cancer cells continue to proliferate uncontrollably and anarchic which leads to an imbalance between cell proliferation and cell death. A tumor cell can mutate in two ways: the signals telling cells not to divide are turned off or the signals telling cells to begin dividing are left on continuously [20]. The NK cells recognize and kill cancer cells and wait for the development of the complementary adaptive immune response. In contrast to the innate immunity, the specific defense mechanism is based on specific recognition of the infectious agent. Specific immunity has a different mode of action for each infectious agent, a variety of immune cells intervene to destroy abnormal cells, note in this regard the cytotoxic T lymphocytes (CTL), which play a central role in the specific immunity. In the case of solid tumor, T cells circulate by the peripheral vessels and colonize the tumor [3], they stop once they induce tumor cells death. When the tumor cells in the peripheral regions are eliminated, the T cells regain their mobility and look for a live tumor cells in the deeper regions of tumor. This sequential repetition "static cytotoxicity/ mobility" leads to the infiltration and the gradual elimination of the tumor, from the periphery to the center [3]. T cells kill the target cells in different ways: they can put signals that lead to the target apoptosis, or they can bind to the Fas ligand on the target surface and causing its apoptosis [13].

The growth and development of solid tumors take place in two distinct stages: the avascular growth phase and the vascular growth phase [7]. Each stage is an important indicator of tumor development, its aggressiveness and the choice of its treatment. Generally, tumor sets out avascular, the nutrients necessary for its growth are supplied via diffusion from distant blood vessels [12]. In addition of its rapid proliferation, tumor develops its own blood system by the process of angiogenesis, otherwise it stays dormant. In order to accomplish its neovascularization, tumor secretes chemical substances into the surrounding tissues to activate a blood support. Several studies have been done to know the nature of these substances and their effect on the endothelial cells since the first research of [18]. The second phase of tumor growth is when the tumor is attaches to a blood vessel. The blood vessel penetrates into the tumor mass and provide it with a constant source of nutrients which leads to a new lease of tumor life in new neighboring tissues and creates more metastases [23]. Tumors develop various strategies to escape immune surveillance [10], which makes the immune cell's mission difficult and sometimes ineffective in eradicating the cancerous cells. When the tumor reaches this stage, treatment should step in.

Immunotherapy is one of the most recent approaches to cancer therapy, it is based on stimulating the body's defenses against cancer cells with activators. One such activator is interleukin-2 (IL-2) which is the main cytokine responsible for the activation of lymphocytes. IL-2 is produced by CD4+T cells and by CD8+T (CTL) cells and NK in lesser quantities. The types of cancers treated in general with immunotherapy by continuous infusion or injections of IL-2, are the renal carcinomas and some types of melanomas. For this reason, the simulated patterns in our work may refer to the growth of renal cell carcinoma or melanoma. Several lines of evidence suggest that the use of immunotherapy with the cytokine IL-2 can boost the immune system to fight cancer. The use of the interleukin-2 on human and animal immune system was studied by Rosenberg et al. [46], the experiments have demonstrated that IL-2 partially restores the immune deficiencies and immune response, it allows the generation of lymphokine-activated killer cell (LAK) and stimulates the activated T cell migration. IL-2 improves also the activity of CTL in different stages of the disease [25,43,49,50] and promotes CTL proliferation [30], also increases the NK cells cytotoxicity [8,40,53]. Experimental studies on animals [26,34,37] and humans [47] have shown that treatment

with maximal dose of IL-2 could produce regression of the tumor but it has a variety of toxic effects that limit its use. The usage of IL-2 with low-dose has double benefits, it enhances the anti-tumor action of IL-2 and at the same time minimizes its toxicity. In [46] trials, the administration of IL-2 at low doses had no side effects and could also lead to the regression of tumor for patients with melanoma and renal carcinoma for different ways of IL-2 administration, only or in combination with LAK.

## CA Rules

In our previous work [56], a free avascular cancer growth was simulated, including tumor cell proliferation, motility and death in the absence of an immune response. In this work, the interaction between tumor cells and immune system will be presented, in addition to the immunotherapy effect. The simulation starts with one tumor cell in healthy tissue. The tissue is represented by a square lattice of size $(L+1) \times (L+1)$, any site, with coordinates $x = (i, j), i, j = 0, 1, 2, \ldots, L$, is occupied by only one of cell types: healthy cell, immune cell (NK or CTL) or tumor cell which may pile up with other tumor cells at the same site. Each cellular automata grid element is assumed to correspond in size to 10 μm, the real biological size cells (10–20 μm [2,31]), with 1 tumor cell = 10 μm = 0.001 mm. The tissue is supplied with his own capillary vessel localized at the top of the lattice at $x = 0$, as well as the capillary vessel of his neighboring tissue at the bottom of the lattice at $x = L$, these vessels are the only source of nutrient for all cells of the tissue. The nutrient elements are supposed divided into two groups: nutrients essential for cell proliferation and nutrients essential for cell survival. The both nutrient types are diffused continuously from the distant capillary vessels throughout the tissue and are consumed by all tissue cells. The nutrient species obey the following deterministic PDEs given by [17] and developed by [32], which present the continuous vessel diffusion:

$$\frac{\partial N}{\partial t} = \nabla^2 N - \alpha^2 (H + I) N - \lambda_N \alpha^2 T N \tag{1}$$

$$\frac{\partial M}{\partial t} = \nabla^2 M - \alpha^2 (H + I) M - \lambda_M \alpha^2 T M \tag{2}$$

where $N$ is the nutrient essential for cell proliferation, $M$ is the nutrient essential for cell survival, $H$ is the total number of normal tissue cell, $I$ is the total number of immune cell and $T$ is the total number of tumor cell, $\alpha$ is the rate of consumption of nutrient by host and immune cells, $\lambda_N$ is the excess consumption factor of N nutrient by tumor over non-tumor cells, $\lambda_M$ is the excess consumption factor of M nutrient by tumor over non-tumor cells. The boundary conditions on the capillary vessels are: $N(0, y) = M(0, y) = 1$, $N(L, y) = M(L, y) = 1$. The periodic boundary conditions along the x-axis are: $N(x, 0) = M(x, 0) = 1$, $N(x, L) = M(x, L) = 1$. The Neumann boundary conditions $\frac{\partial N(L,y)}{\partial t} = \frac{\partial M(L,y)}{\partial t} = 0$, are imposed to the border of the tissue (Fig. 1). All parameters are presented in Table 1. Probabilistic rules is used in order to assign the stochastic nature of the tumor–immune interaction.

### *Tumor Cells*

At each temporal iteration, which corresponds to the division cycle of tumor (a period of approximately 0.5–10 days, it depends on the cell type in question [25,44]), each cancer cell can divide, migrate or die. A random number is chosen at each grid point and compared to the calculated probability values to determine the action that will be carried out.

**Table 1** Variables and model parameters

| Variable | Description |
|---|---|
| $N(x, y, t)$ | Proliferation nutrient concentration |
| $M(x, y, t)$ | Survival nutrient concentration |
| $H$ | Normal cell number |
| $T$ | Tumor cell number |
| $I$ | Immune cell number |
| $D$ | Interleukin-2 concentration |
| **Parameter** | **Description** |
| $\alpha$ | Rate of consumption of nutrient by host and immune cells |
| $\lambda_N$ | Excess consumption factor of tumor over non-tumor cells of N nutrient |
| $\lambda_M$ | Excess consumption factor of tumor over non-tumor cells of M nutrient |
| $P_{div}$ | Probability of tumor cell division |
| $P_{mov}$ | Probability of tumor cell migration |
| $P_{dth}$ | Probability of tumor cell death |
| $P_{imdth}$ | Probability of tumor cell death due to the immune system |
| $P_{nk}$ | Probability of the production of a new natural killer cell |
| $P_{ind}$ | Probability of induction of a CTL due to CTL/T interaction |
| $P_{Dctl}$ | Probability of CTL death |
| $P_{PL}$ | Probability of CTL proliferation due to IL-2 injection |
| $\theta_{div}$ | Shape parameter for cell division probability curve |
| $\theta_{mov}$ | Shape parameter for migration probability curve |
| $\theta_{dth}$ | Shape parameter for death probability curve |
| $\theta_{ind}$ | Shape parameter for CTL induction probability curve |
| $\theta_{Dctl}$ | Shape parameter for CTL death probability curve |
| $\theta_{PL}$ | Shape parameter for CTL proliferation probability curve |
| $I_0$ | Level of natural killer cells |

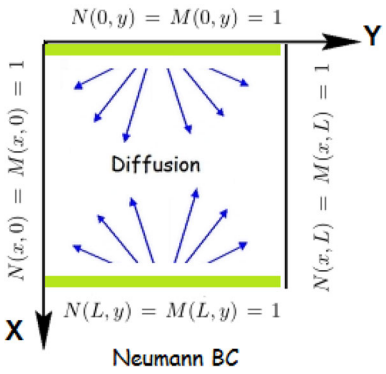


**Fig. 1** Schematic of the cellular automata. The conditions imposed on the boundaries are indicated

*Division:* For a selected tumor cell, the chance of division increases with the ratio of nutrient concentration essential for cell proliferation to the number of cancerous cells. If the selected cell is inside the tumor, the daughter cell will occupy the same mother site, they pile up at

that site. If the selected cell is on the tumor border, his daughter will occupy randomly the nearest site containing a normal or a necrotic cell. The probability form of cell division used by Ferreira et al. [17] is:

$$P_{div} = 1 - \exp\left[-\left(\frac{N}{T\theta_{div}}\right)^2\right] \tag{3}$$

*Migration:* A tumor cell may migrate when the number of cancerous cells in its microenvironment is high due to the competition between cells for nutrients. It is also possible that a tumor cell moves from the areas in which the concentration of nutrients is low, or when the level of concentration of essential nutrients necessary for survival is high, possibly because nutrients promote the cell migration. The probability term proposed by [17] adopts the third viewpoint, which is given by:

$$P_{mov} = 1 - \exp\left[-T\left(\frac{M}{\theta_{mov}}\right)^2\right] \tag{4}$$

If the selected cell is inside the tumor, it will move to a nearest neighbor site chosen at random. If the selected cell is on the tumor border and there is no other cells in the same site, it will migrate by interchanging its position with the position of a normal cell. If the selected cell is on the tumor border and there is another cell in the same site, then it will occupy the position of nearest normal or necrotic cell.

*Death*: A tumor cell may die in two different ways: the nutrient elements are insufficient, in this case the probability term used by Ferreira et al. [17] is given by:

$$P_{dth} = \exp\left[-\left(\frac{M}{T\theta_{dth}}\right)^2\right] \tag{5}$$

This probability term implies that for a tumor cell, the chance to die increases as the ratio of the nutrient $M$ to the number of tumor cells decreases. Tumor cell may die also due to the immune cells, the probability term proposed by Mallet et al. [32] is given by:

$$P_{imdth} = 1 - \exp\left[-\left(\sum_{j\in\eta} I_j\right)^2\right] \tag{6}$$

This probability term takes into account the strength of the local immune system in the tumor cell's neighborhood which is considered as a major factor in tumor death processes. In other words, the probability of tumor death increases as the number of neighboring immune cells increases. The summation counts the total number of immune cells in the neighborhood $\eta$ (the eight CA surrounding element $j$ of the current tumor cell).

*Immune Cells*

*NK cell production*: When cancerous cells divide, the immune cells intervene and NK cells are the first line of defense. It is assumed that the number of NK cells is stable around a constant $I_0$ in order to keep a normal level of NK cells, where $I_0 n^2$ is the number of the Nk cells placed over the tissue. Mallet et al. [32] have proposed a form of birth as a probabilistic term of natural killer cell's production $P_{nk}$. At each time step and for all grid site, a random number is compared with $P_{nk}$, if the random number is less than $P_{nk}$ and the grid element

is not occupied by a tumor cell, than a NK cell will be placed in that element. This strategy aims to allow the NK cells to come in open spaces such as from the below of the grid or the space near to the blood vessel. The probability of NK cell production is given by:

$$P_{nk} = I_0 - \frac{1}{n^2} \sum_{i,j=0,0}^{n,n} I_{i,j} \tag{7}$$

where $n^2$ is the size of the square domain and the summation counts the number of NK cells in all CA.

*CTL induction:* It is considered that the CTL cells will be recruited to the tumor location in two different ways. Firstly, when NK cell comes in contact with a tumor cell it is possible that the tumor cell will be killed and the NK cell will be destroyed also with the tumor cell, in this case NK grid place will signal the CTL induction at the next time step. Secondly, the induction processes will also be initiated when a CTL cell comes in contact with a tumor cell, the surrounding CA elements signal the CTL induction. The probability term for CTL induction proposed by Mallet et al. [32] is given by:

$$P_{ind} = \exp\left[-\left(\frac{\theta_{ind}}{\sum_{j\in\eta} T_j}\right)^2\right] \tag{8}$$

For each neighboring cell, a random number is compared with $P_{ind}$ to determine if the induction will be carried out or not. The summation counts the number of tumor cells in the neighborhood $\eta$ of the current CA element. $P_{ind}$ is defined to be equal zero if there are no tumor cells nearby.

*Immune cell death:*

- If the immune cell is NK cell, then it will be dying when it is in contact with a tumor cell.
- If the immune cell is CTL cell, it is assumed to die if no tumor cells are detected in its neighborhood, this death take place with a probability suggested by Mallet et al. [32] such as:

$$P_{Dctl} = 1 - \exp\left[-\left(\frac{\theta_{Dctl}}{\sum_{j\in\eta} T_j}\right)^2\right] \tag{9}$$

The summation count the total number of tumor cells in the neighborhood of CTL cell. The probability is defined to be unity when there are no neighboring tumor cells.

*Immune cell migration:* As well as the tumor cell is not found, the immune cells continue to move randomly towards the grid element, once they find cancer cells they will intervene to eradicate one at random.

## Immunotherapy Intervention

In general, immunotherapy may be used as an attack treatment (general treatment) for all of the body, by injecting the system with the immune system activators such as IL-2, with a continuous perfusion or injections. The treatment with IL-2 alone or in conjunction with other therapy has produced beneficial effects in the treatment of metastatic melanoma [51]

and metastatic renal cancer [55]. Immunotherapy can be also used in preventive fashion, to prevent the recurrences after a surgery ablation, in this case the treatment is local and the immunity is stimulated only locally. This kind of treatment may be taken for the bladder and the cervical cancers. Immunotherapy treatment is based on a clinical staging which depends on whether cancer has spread to regional lymph nodes or distant sites. It may be taken every day, week, or month, some immunotherapies are given in cycles followed by a period of rest.

IL-2 doses are adjusted for the size of the patient body, either his weight in kilograms, in this case the amount of a dose will be given in milligrams of drug per kilogram of body weight abbreviated mg/kg (or IU/kg). Or by measuring the body surface area (BSA). BSA is measured in square meters, abbreviated $m^2$, in this case the amount of a dose will be given in milligrams of drug per square meter abbreviated mg/$m^2$ (or IU/$m^2$) [14].

The administration of IL-2 depends on the type of cancer and how advanced it is, the type of immunotherapy and how the body reacts to treatment. The optimum dose of IL-2 is unknown, it is generally administrated for metastatic renal cell carcinoma and metastatic melanoma such that: 600,000 IU/kg (0.037 mg/kg) *IV* over 15 min every 8 h for a maximum of 14 doses, then 9 days of rest, then a maximum of 14 more doses [9]. IL-2 can be taken in higher or lowest doses, the high-dose therapy appears to be associated with higher response rates but with more toxic effects. The low-dose of interleukin-2 is usually given as a shot under the skin (subcutaneous injection), in some situations, patients may be able to give themselves these injections at home.

For renal cell cancer, the high-dose used in [19] is the most used regimen in the United States. This therapy consists of 600,000–720,000 IU/kg administered over a time frame of 15 min by *IV* bolus every 8 h. A course consists of a maximum of 14 doses in 5 days, then the patient rests for 5–9 days. Courses are repeated every 6–12 weeks. In contrast, the low dose used in [55] is 72,000 IU/kg administered by *IV* bolus every 8 h. A course is up to 14 doses in 5 days, which is followed by a rest period of 7–10 days. Courses are repeated every 8 weeks. For melanoma, there are several treatment methods which have advantages and disadvantages. In the Rosenberg scheme [48], IL-2 is given in high doses (50–70 million units/$m^2$/day). In the West Scheme [54], IL-2 is administered to intermediate dose (18 million units/$m^2$/day by continuous perfusion).

In this work, the immunotherapy is used as an attack treatment in low doses, four injections, four times per week during 18–27 weeks. The administration of IL-2 at low doses in long term, has no side effects and leads to the regression of tumors [46]. It is assumed in our simulations that when the tumor size reaches 7 mm, the immunotherapy treatment with IL-2 starts. In addition, we simulate other cases when the immunotherapy starts for tumors reaching 300, 500 or 900 mm. At these tumor sizes and beyond 2 mm, the tumor has already developed his blood circulation by the process of angiogenesis [38]. For this reason, we will consider that their is a third capillary vessel which is developed by the angiogenesis process and provides nutrient elements to the tumor (it is not visible in the simulation patterns, but it is considered in our mathematical calculations).

IL-2 Joins the blood via absorption and get dispersed by blood circulation throughout the body, then reaches various parts of the system via blood vessels, and finally get diffused into targeted organs via capillary vessels [39]. In our immunotherapy simulations the low dose of IL-2 is equivalent to the low diffusion of IL-2 by the capillary vessels. We consider a diffusion equation of IL-2 where the first term represents the diffusion of IL-2, and the second serves as a consumption term of IL-2 by immune cells as follow:

$$\frac{\partial D}{\partial t} = \nabla^2 D - \alpha^2 I D \tag{10}$$

The boundary conditions are: $D(0, y) = D_0$, $D(L, y) = D_1$, $D(x, 0) = D_2$, $D(x, L) = D_3$.

When it corresponds to the day of injection, the concentration of IL-2 is calculated to determine the low dose of IL-2 diffused into the tissue. The immune cells localized on high IL-2 concentration area have the best chance to benefit from this stimulator treatment. When it is the day of rest and there is no injection to take, IL-2 concentration is assumed to be equal to zero.

As it is described in "Biological Background" section, the use of immunotherapy with IL-2, promotes CTL proliferation and increases the NK cell cytotoxicity. We introduce the IL-2 effect on CTL cells to the model by adding a probabilistic term of CTL cell proliferation due to IL-2 injections as follows:

$$P_{PL} = 1 - exp\left[-\left(\frac{D}{(Nb_{ctl})\theta_{PL}}\right)^2\right] \tag{11}$$

where $Nb_{ctl}$ is the number of CTL cells in all of the grid, $\theta_{PL}$ is the shape parameter for CTL proliferation probability curve. This probability term implies that for a CTL cell, the chance of proliferation increases with the ratio of interleukin-2 concentration $D$ to the number of CTL cells.

After the IL-2 injection, the NK cell cytotoxicity enhances, we simulate this effect of IL-2 on NK cells, at the NK cell death level. We assume that during the immunotherapy treatment, the NK cells don't die along with tumor cell in their first contact, but they adopt such a competence to destroy more than one cancerous cell, we use $k$ to represent the number of tumor cell killed, with $k \leq 2$.

## Simulation and Results Without Immunotherapy Intervention

### Algorithms

The basic outline of the code can be summarized through the following stages:

1. Construct the data structures.
2. Get parameters and assign values.
3. Initialize system, the cellular automata configuration starts with one tumor cell in the middle of the grid,
4. Solve the diffusion equations in the steady- state, to obtain initial nutrient concentrations.
5. Begin for-loop
   - Assign random numbers to all CA sites for use in next cell action.
   - For each selected cancer or immune cell, calculate probabilities to define the cell action (tumor division, tumor or immune migration, tumor or immune death, CTL cell induction, NK cell production).
   - Move immune cells around.
   - Regenerate NK cells as needed.
   - Update the CA structure according to the changed states.
   - Recalculate nutrient element distributions.
   - If ((the tumor size reaches 7 mm) or (the immunotherapy is started)) and (the duration of therapy is not yet finished) then
     - Calculate the immunotherapy chemical diffusion equation.

– Test the end conditions (until reaching the final time).

End for-loop

6. Plot the results.

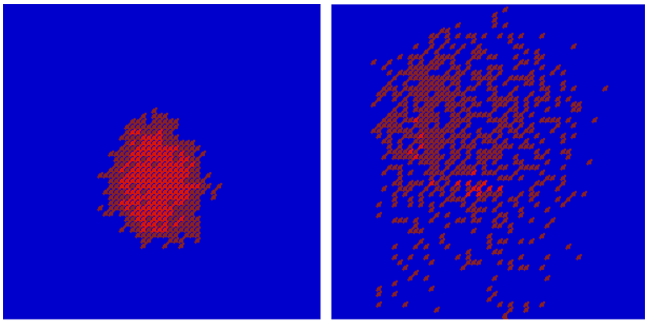


**Fig. 2** Tumor morphology at the end of a simulation. **a** Parameter values are: $\alpha = 1/L, \lambda_N = 100, \lambda_M = 10, \theta_{div} = 0.3, \theta_{mov} = 10000, \theta_{dth} = 0.01$. **b** Parameter values are: $\alpha = 2/L, \lambda_N = 25, \lambda_M = 10, \theta_{div} = 0.3, \theta_{mov} = 0.1, \theta_{dth} = 0.01, I_0 = 0.02$. **a** Compact morphology. **b** Disconnected morphology

## Tumor Morphology

One of the main tumor characteristic is the morphology, which may be affected by several factors. In [17] work on free growth of an avascular tumor (without immune response intervention), the nutrient consumption by normal and cancer cells, controlled by the model parameters $\alpha$, $\lambda_N$ and $\lambda_M$, played an important role in morphology determination and correspond to the competition between normal and tumor cells for nutrients. The simulated patterns were compact for low $\alpha$ values and lowest $\lambda_N$ and became papillary for high $\lambda_N$, and more papillary for higher $\alpha$. This results were investigated in [32] and have taken into consideration the immune system response. Another factor has studied in [16] which played a central role in tumor morphology, the simulations showed that for low cell motility probability the simulated patterns were compact. In contrast, for high cell motility probability the simulated patterns were disconnected and tumor cells were dispersed on the tissue.

In this work, two types of tumor morphology are studied, the compact morphology and the disconnected morphology as it is shown in Fig. 2. For low consumption rate of nutrient $\alpha$ and for $\lambda_N$=100 and with low cell migration, the tumor morphology is compact, which may be explained by the low competition between tumor and normal (healthy and immune) cells for nutrients. For high $\alpha$ value and with the cell migration process, the tumor morphology is disconnected, the cancerous cells are dispersed due to the high competition, and they keep looking for nutrients throughout the tissue.

## The Immune System Effectiveness

When the immune system fights tumor on his own, in the absence of therapeutic intervention, his effectiveness depends on his strength, his ability to recognize cancerous cells and his response to destroy tumor. In this section, tumor–immune interaction in the absence of immunotherapy is presented, the CTL recruitment parameter is used as an indicator of strong or weak immune system.

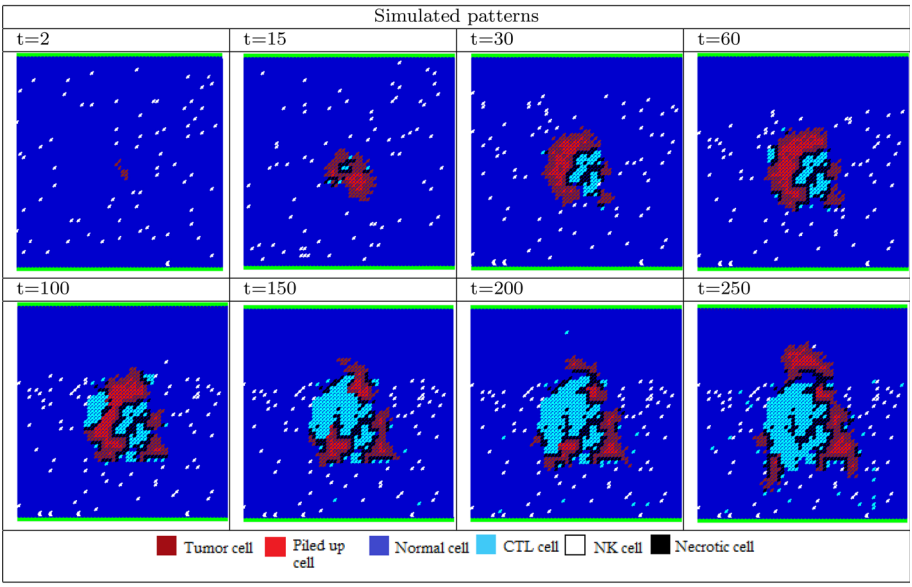


**(a)**

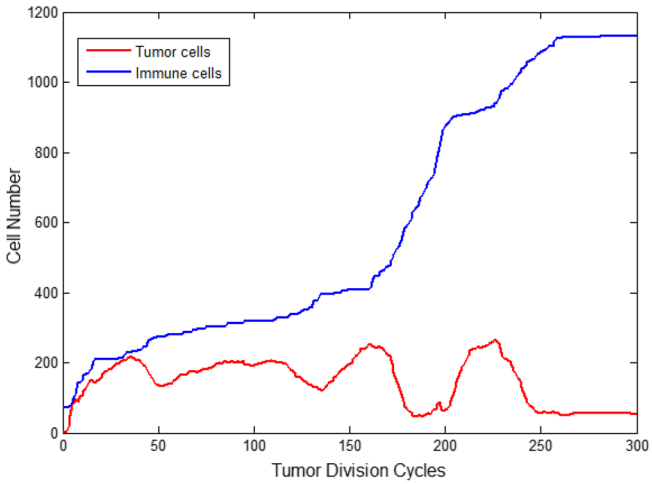


**(b)**

**Fig. 3** The effect of high CTL induction on tumor and totlal (NK + CTL) immune cell over time. Parameter values are: 60×60 square lattice, $\alpha = 1/L$, $\lambda_N = 100$, $\lambda_M = 10$, $\theta_{div} = 0.3$, $\theta_{mov} = 10000$, $\theta_{dth} = 0.01$, $\theta_{ind} = 2$, $\theta_{Dctl} = 0.3$, $I_0 = 0.02$

### *High CTL Induction*

For high CTL induction, which corresponds to the lowest value of $\theta_{ind}$, tumor cell population shows few oscillations without exceeding 200 cells, while the immune cell population increases over time, as shown in Fig 3b. A strong immune system may eradicate or keep the tumor mass in controls in the absence of therapeutic intervention. Two-dimensional illustra-

tion of tumor–immune interaction at several times of simulation with high CTL induction are shown in Fig 3a. The parameters of the compact-tumor are used in this simulation. Similar results were observed in simulations using disconnected-tumor parameters.

*Low CTL Induction*

For low CTL induction, which corresponds to the higher value of $\theta_{ind}$, tumor cell population grows over time, while the immune cell population remains low due to the low recruitment of CTL cells as shown in Fig 4b. Two-dimensional illustration of tumor–immune interaction at several times of simulation with low CTL induction is shown in Fig 4a. In this case, the immune system alone is not sufficient to eradicate tumor cells in the absence of therapeutic intervention. The parameters of the compact-tumor are used in this simulation. Similar results were observed in simulations using disconnected-tumor parameters. In "Simulation and Results with Immunotherapy Intervention" section, we introduce the immunotherapy with IL-2 to the low CTL induction case in order to stimulate the immune system against the cancerous cells.

### The Growth Curve

All tumors follow a standard growth pattern, growing fastest in the beginning and eventually reaching a maximum size. The exponential growth model fails to model this behavior in vivo, while the Gompertz model [27] is type of models where growth is slower at the end of a time period. In [17] , the progress on time of the tumor cells population follows the Gompertz curve, which has the functional form as follow:

$$N_C(t) = A \exp[-\exp(-B(t - t_c))] \tag{12}$$

where $N_C(t)$ is the total number of tumor cells present at time t, the parameters $A$ and $B$ evaluated by the least-square methods. In [32], the tumor cells population has not a functional form. In our simulations, also the tumor cells has not a functional form and the total number of tumor cells increases as long as the tumor cells divide, and decreases when they died. The simulated tumor growth curve and the fitted Gompertz function are represented in Fig 5c.

## Tumor Characteristics Obtained from the Growth Patterns

We aim to extract some tumor characteristics from the simulated tumor growth patterns such as tumor fractal dimension, the fractality of the boundary and the number of cells on tumor periphery. We discuss their biological implications and we evoke the experimental results and observations for tumor growth of other researchers.

### Tumor Fractality

Tumor growth can be described in terms of mathematical models from different points of view, such as exploiting the geometrical features of growth, using the theory of fractal geometry. One of the characteristics of cancerous tumors is the extreme irregularity of their boundaries, it is an important prognostic indicator of tumor invasion and dynamic behavior of tumor (Keefe et al. 1990). Thus, the oncologists have posed the problem of finding a mathematical tool to quantify the irregularity of cancerous tumors. This tool is fractal dimension (a measure of complexity degree). The concept and measurement of fractal dimension by using the

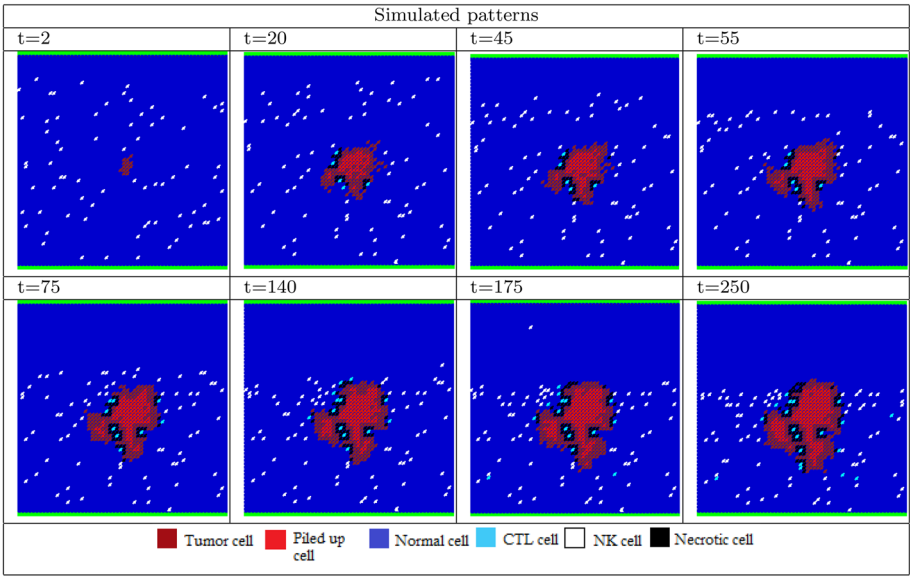


**(a)**

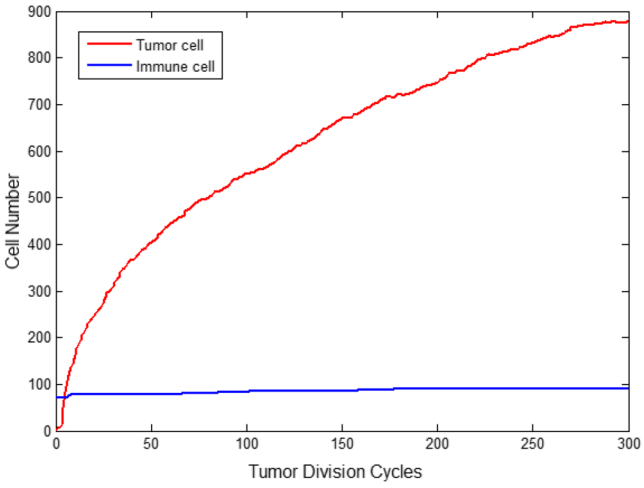


**(b)**

**Fig. 4** The effect of low CTL induction on tumor and total (NK + CTL) immune cell over time. Parameter values are: 60×60 square lattice, $\alpha = 1/L$, $\lambda_N = 100$, $\lambda_M = 10$, $\theta_{div} = 0.3$, $\theta_{mov} = 10000$, $\theta_{dth} = 0.01$, $\theta_{ind} = 9$, $\theta_{Dctl} = 0.3$, $I_0 = 0.02$

box-counting method is given by [5,11]. The Box-counting method is useful to determine fractal properties of a 1D segment, a 2D image or a 3D array. An investigation on malignant melanomas has been done by two groups in [11], the study was conducted involving clinical colour photographic slides of 43 melanomas and 45 benign lesions, their results show that the irregularity was a strong discriminating factor to distinguish the benign and malignant melanomas. The fractal dimension of the boundary found was in the range of 1.05–1.30.

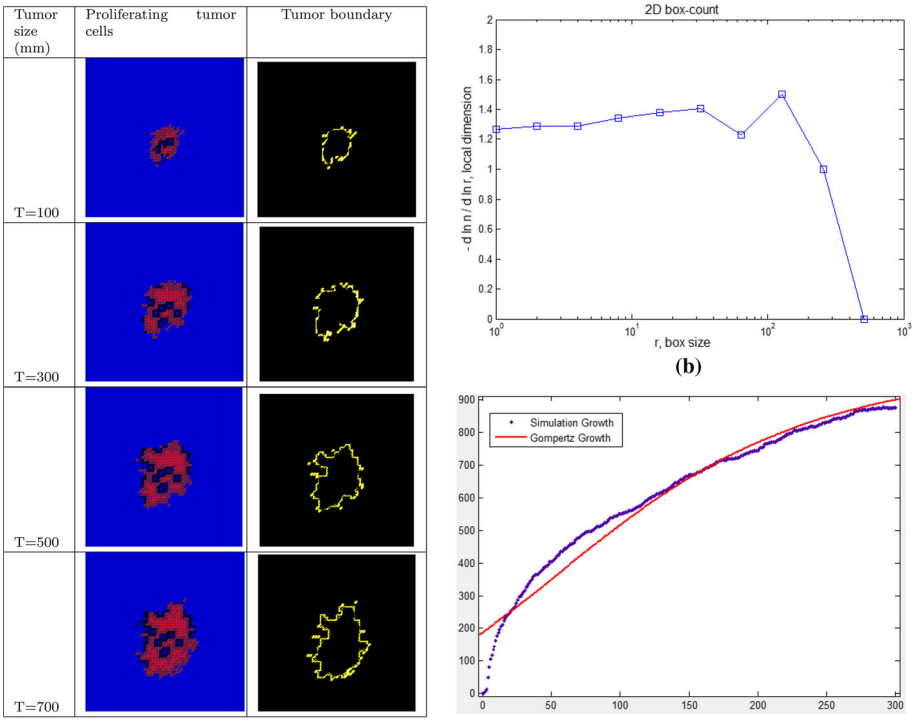


**Fig. 5** **a** Simulated tumor growth on a $60 \times 60$ square lattice, the proliferating cell of the tumor and its boundary. **b** Fractal dimension by using the box-counting method. **c** Simulated tumor growth curve with the fitted Gompertz growth function. Parameter values for the simulated tumor growth are: $60 \times 60$ square lattice, $\alpha = 1/L$, $\lambda_N = 100$, $\lambda_M = 10$, $\theta_{div} = 0.3$, $\theta_{mov} = 10000$, $\theta_{dth} = 0.01$, $\theta_{ind} = 2$, $\theta_{Dctl} = 0.3$, $I_0 = 0.02$. The best fitting is obtained for the parameters $A = 860.2748$ and $B = 0.0094$

Bru et al. [5] have worked on human and animal solid tumors in order to analyze the fractal nature of 16 types of human tumors, which were surgically removed from patients and developed in vivo (the tissue sections were 4 μm thick), their experimental data found for the fractal dimension boundary of tumors was in the range of 1.09–1.34. Landini et al. [28] and [29] have studied a dysplastic and malignant epithelial lesions in the oral cavity using a complex method of fractal analysis, the range of fractal dimensions was wide 1.00 for normal epithelium to 1.61 for invasive carcinoma. In [16], a model for the growth of primary carcinoma, including cell proliferation, motility and death. The fractal dimension found increases as well as the total number of tumor cells increases too. We define the boundary cells of simulated solid tumor, assuming that they are the outermost tumor cells which have at least a normal neighboring cell as it is shown in Fig 5a. Our fractal dimension of simulated tumor boundaries in time steps 300 is 1.24 as it is exhibited in Fig 5b, where $n$ represents the number of squares needed for a fractal shape to be completed, $r$ is the respective square size. The value of fractal dimension $FD$ of the shape corresponds to the value where the first derivative $-\frac{d\ln(n)}{d\ln(r)}$ remains constant for a space of $r$ [35]. In addition, we notice that the fractal dimension increases as well as the total number of tumor cells increases too, this observation is consistent with [16] observation for primary carcinoma growth.

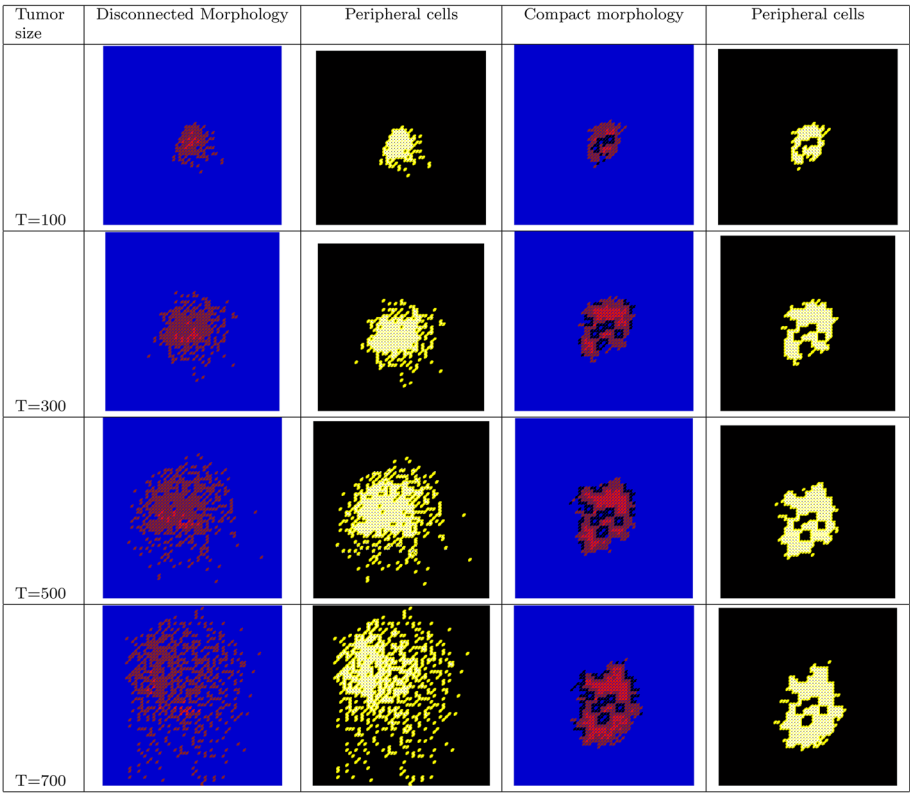


**Fig. 6** Simulated tumor growth on a $60 \times 60$ square lattice and their peripheral cells (*yellow color*). Parameter values for the disconnected morphology are: $\alpha = 2/L$, $\lambda_N = 25$, $\lambda_M = 10$, $\theta_{div} = 0.3$, $\theta_{mov} = 0.1$, $\theta_{dth} = 0.01$, $\theta_{ind} = 9$, $\theta_{Dctl} = 0.3$, $I_0 = 0.02$. Parameter values for the compact morphology are: $\alpha = 1/L$, $\lambda_N = 100$, $\lambda_M = 10$, $\theta_{div} = 0.3$, $\theta_{mov} = 10000$, $\theta_{dth} = 0.01$, $\theta_{ind} = 9$, $\theta_{Dctl} = 0.3$, $I_0 = 0.02$

## Number of Cells on Tumor Periphery

One of the characteristics of a tumors is the number of cancer cells in their periphery. These cells are in contact with the healthy environment where oxygen is not lacking, and where they divide continuously. The peripheral cells in our simulations are defined as the outermost tumor cells which have at least a normal neighboring cell as it is viewed in Fig 6. We notice that the peripheral cells in this work depend on cell motility. For low cell motility, the number of times that the tumor migration probability $P_{mov}$ is carried out over the CA configurations is near or equal to zero as it is shown in Fig 7c, the patterns morphology are compact from the beginning, which explain the small number of the peripheral cells as it is shown in Fig 7d. While, for high cell motility, the number of times that the tumor migration probability is carried out over the CA configurations is high as it is shown in Fig 7a, the growth patterns are constituted by single cells highly dispersed on the tissue and the great majority of them are in the tumor outermost region, which explain the high number of the peripheral cells as it is shown in Fig 7b. Our observations are in good agreement with [16] for primary carcinoma growth.

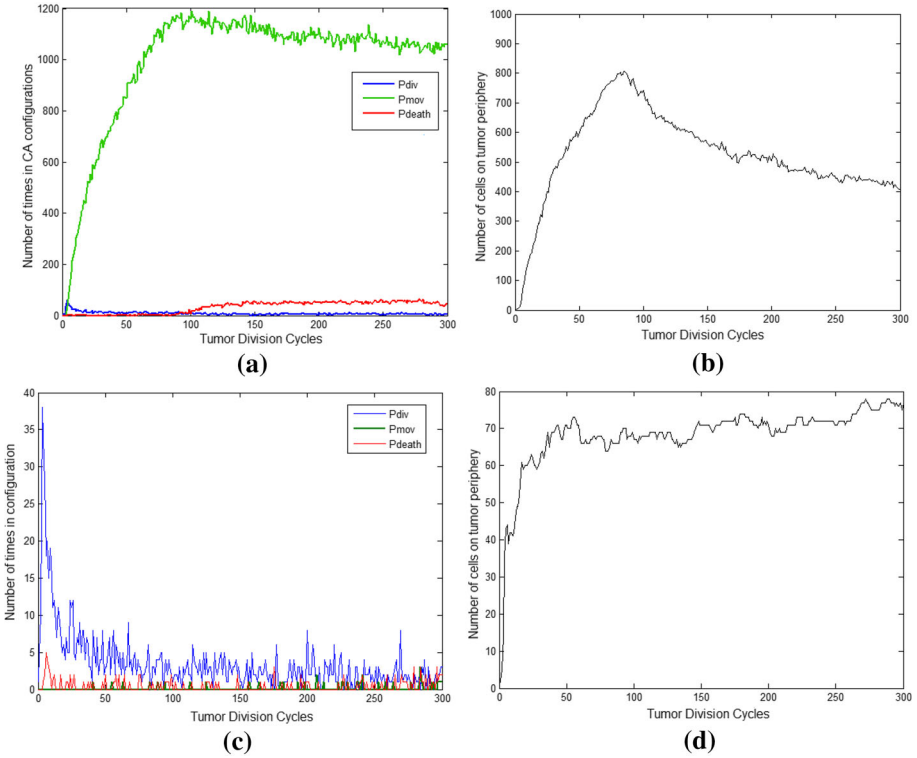


**Fig. 7** Disconnected morphology: **a** Number of times that every probability (division, migration, death) is carried out. **b** Number of cells on tumor periphery. Parameter values are: $\alpha = 2/L$, $\lambda_N = 25$, $\lambda_M = 10$, $\theta_{div} = 0.3$, $\theta_{mov} = 0.1$, $\theta_{dth} = 0.01$, $\theta_{ind} = 9$, $\theta_{Dctl} = 0.3$, $I_0 = 0.02$. Compact morphology: **c** Number of times that every probability is carried out in CA configurations. **d** Number of cells on tumor periphery. Parameter values are: $\alpha = 1/L$, $\lambda_N = 100$, $\lambda_M = 10$, $\theta_{div} = 0.3$, $\theta_{mov} = 10000$, $\theta_{dth} = 0.01$, $\theta_{ind} = 9$, $\theta_{Dctl} = 0.3$, $I_0 = 0.02$

## Simulation and Results with Immunotherapy Intervention

In this section, we simulate the immunotherapy with IL-2 administered into the body after the tumor is large enough to be detected and has already develop his blood vessel. The immunotherapy is used for the low CTL induction case ("Low CTL Induction" section), where the body alone cannot eliminate the tumor cells. We have examined several strategies of the IL-2 administration and we have determined that the tumor mass decreases with remarkable way with 4 injections 4 times per week during 18–27 weeks with low IL-2 doses, which are equivalent to the low diffusion of IL-2 by the capillary vessels. To determine the low diffusion of IL-2 we have used low values of the initial conditions, however, we haven't noticed any changes in our CA. In contrast, we remarked that for the initial condition values: $D_0 = 10^3$, $D_1 = 10^3$, $D_2 = 10^3$, $D_3 = 10^3$, the CTL cells begin to proliferate and as long as we increase the initial condition values, the CTL cells proliferation increases too fast. When it corresponds to the day of injection, we solve the differential equation (10) with the finite difference method in order to determine the low IL-2 concentration. The immune cells localized in high IL-2 concentration areas have the best chance to benefit from the treatment. When it is the day of rest and there is no injection to take, IL-2 concentration is

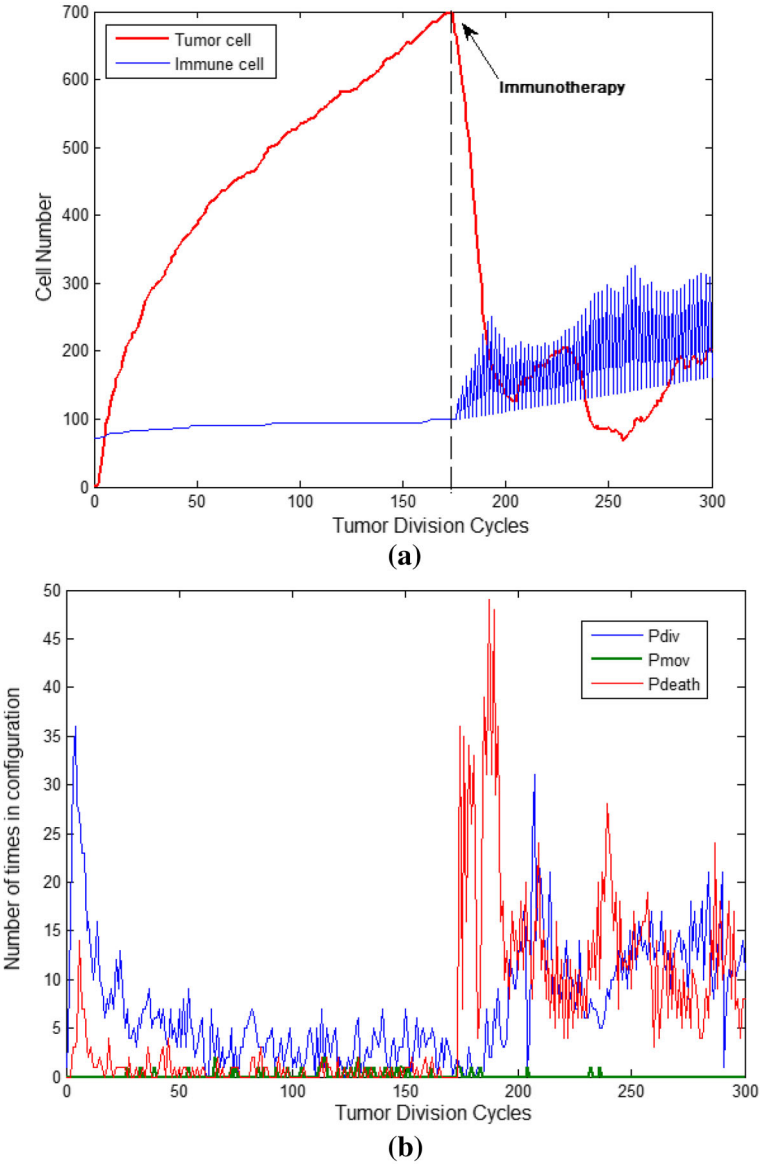


**Fig. 8** The immunotherapy effect on a compact tumor. **a** Tumor and immune cells number before and after immunotherapy intervention. **b** Number of times that every probability (division, migration, death) is carried out in CA configurations. Parameter values are: $60 \times 60$ square lattice, $\alpha = 1/L$, $\lambda_N = 100$, $\lambda_M = 10$, $\theta_{div} = 0.3$, $\theta_{mov} = 10000$, $\theta_{dth} = 0.01$, $\theta_{ind} = 9$, $\theta_{Dctl} = 0.3$, $\theta_{PL} = 0.5$, $I_0 = 0.02$

assumed to be equal to zero. We aim also to show that, cell motility has not only an effect on tumor morphology, but also on the immunotherapy efficiency against cancer. Each temporal iteration corresponds to the division cycle of tumor, a period of approximately 0.5–10 days. In our simulation it is assumed to be 1 day.

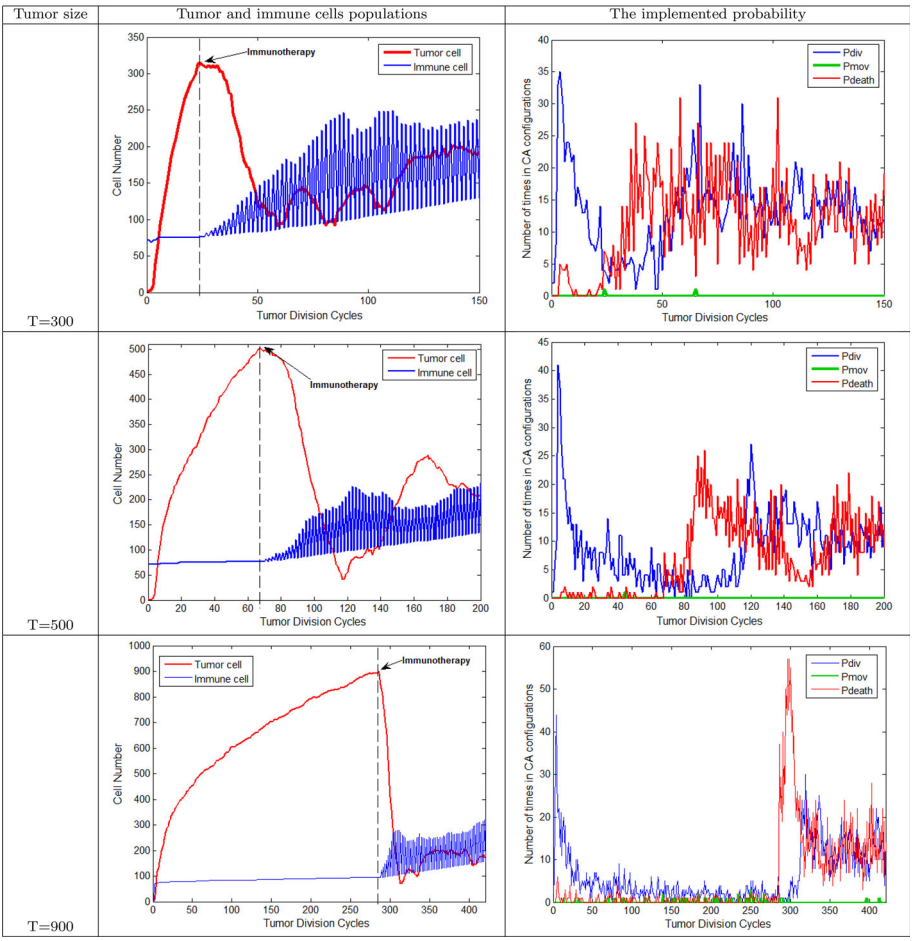


**Fig. 9** The immunotherapy effect on compact tumors reaching different sizes. Tumor and immune cells populations before and after immunotherapy intervention. Number of times that every probability (division, migration, death) is carried out in CA configurations. Parameter values are: $60 \times 60$ square lattice, $\alpha = 1/L$, $\lambda_N = 100, \lambda_M = 10, \theta_{div} = 0.3, \theta_{mov} = 10000, \theta_{dth} = 0.01, \theta_{ind} = 9, \theta_{Dctl} = 0.3, \theta_{PL} = 0.5, I_0 = 0.02$

## Compact Morphology

Before the immunotherapy intervention, the tumor cells grow and invade the tissue and seek to metastasize which leads to an increasing growth curve. In contrast, the immune cells are in low number due to the low induction of CTL as it is noticed in Fig. 8a. This is may be explained by the high number of times that the probability of division was carried out and also the low probability of tumor death due to the immune cells as it is shown in Fig. 8b. Once the tumor reaches 700 cancerous cells, the immunotherapy intervention starts and the tumor cell number decreases with unstable oscillations and stays low, while the immune cell number shows repetitive oscillations during the cure period due to the stimulatory effect of IL-2 injections, which make the probability of tumor death becomes very high during the therapy phase. The tumor cells are under control of the immune system, the oscillation

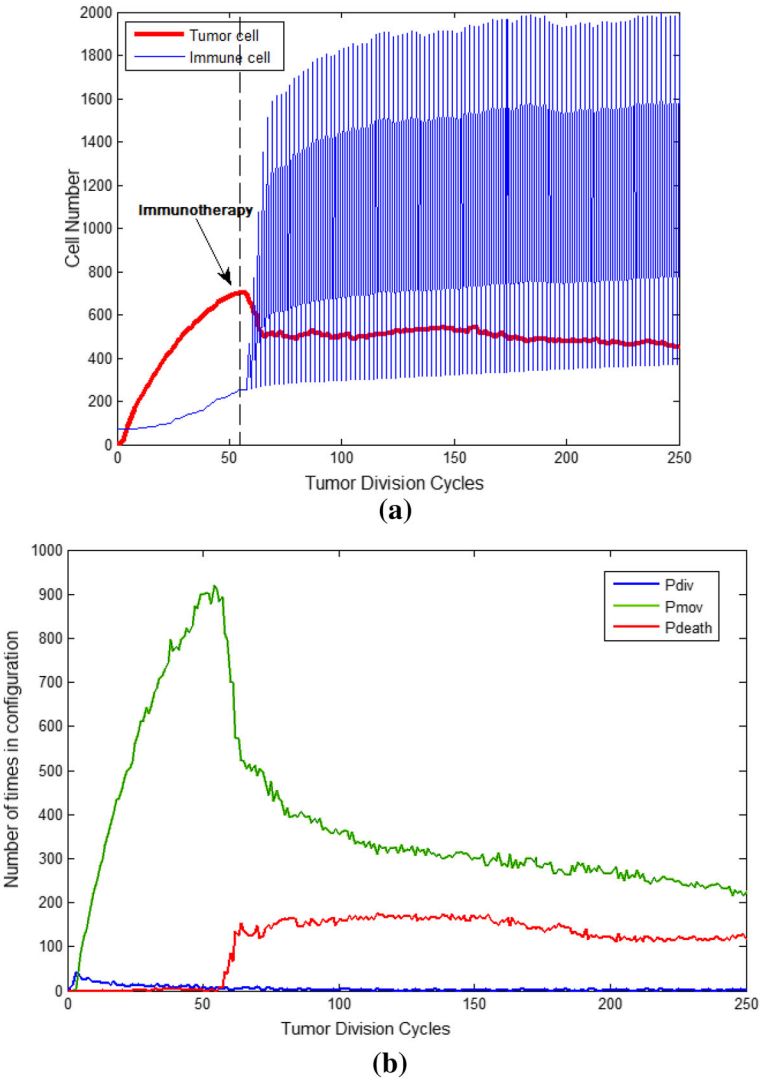


**Fig. 10** The immunotherapy effect on a disconnected tumor. **a** Tumor and immune cells number before and after immunotherapy intervention. **b** Number of times that every probability (division, migration, death) is carried out in CA configurations. Parameter values are: $60 \times 60$ square lattice, $\alpha = 2/L$, $\lambda_N = 25$, $\lambda_M = 10$, $\theta_{div} = 0.3$, $\theta_{mov} = 0.1$, $\theta_{dth} = 0.01$, $\theta_{ind} = 9$, $\theta_{Dctl} = 0.3$, $\theta_{PL} = 0.5$, $I_0 = 0.02$

corresponds to the day of IL-2 injection, which is administered with 4 injections 4 times per week during 18 weeks. The simulation starts with a single mutated cell which divides in the area with a suitable nutrient concentration level. Due to the low induction of CTL and the absence of cell migration, tumor cells keep growing close to each other which leads to compact tumor morphology. Once the tumor size reaches 7 mm, immunotherapy starts and the CTL proliferation are activated as well as the NK cell cytotoxicity, for this reason the tumor mass decreases under his half initial size. The cancer cells try to escape from immune cells, they come closer to the capillary vessel at the end of the simulation. The immunotherapy

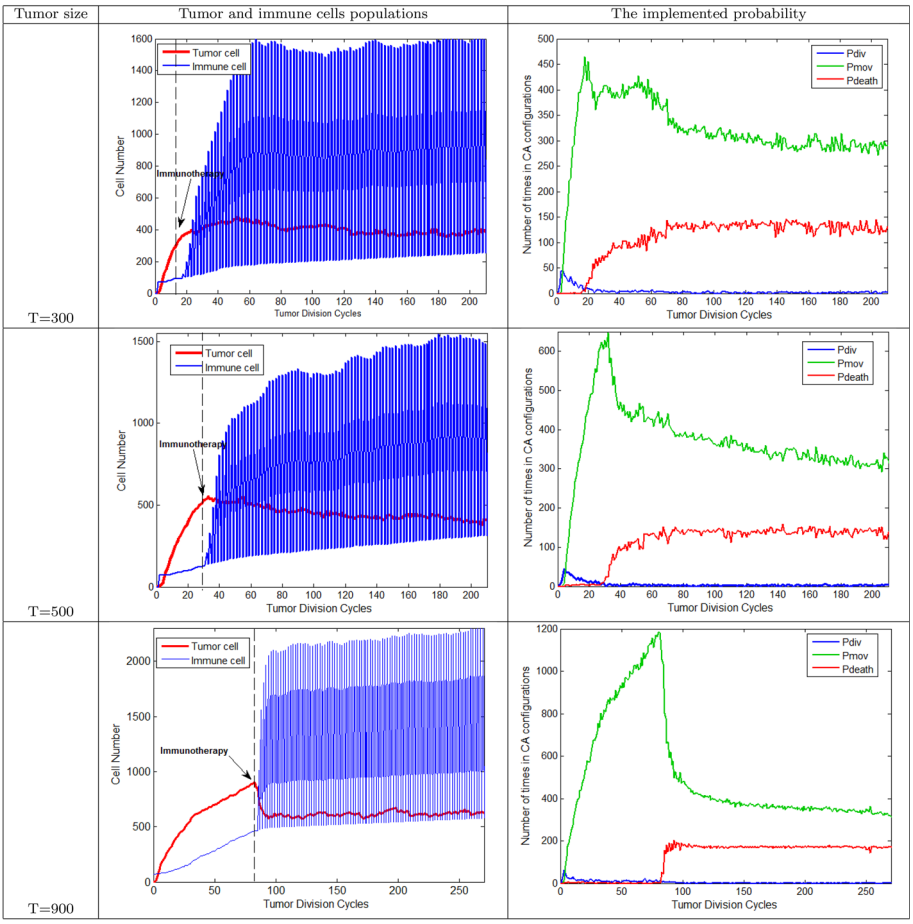


**Fig. 11** The immunotherapy effect on disconnected tumors reaching different sizes. Tumor and immune cells populations before and after immunotherapy intervention. Number of times that every probability is carried out in CA configurations. Parameter values are: $60 \times 60$ square lattice, $\alpha = 2/L$, $\lambda_N = 25$, $\lambda_M = 10$, $\theta_{div} = 0.3$, $\theta_{mov} = 0.1$, $\theta_{dth} = 0.01$, $\theta_{ind} = 9$, $\theta_{Dctl} = 0.3$, $\theta_{PL} = 0.5$, $I_0 = 0.02$

for a compact tumor (low cell migration) was effective in reducing the tumor mass. Several snapshots of simulated tumor–immune and therapy interactions are represented in Fig. 12 and show the declining number of tumor cells. The same results are obtained when the immunotherapy starts for tumors reaching 300, 500 or 900 mm as it is viewed in Fig. 9.

## Disconnected Morphology

Due to the disconnected morphology of the tumor and the dispersed nature of cancerous cells, the tumor grows and reaches 700 cells in a short period as it is shown in Fig. 10a, which leads to 27 weeks of immunotherapy administration. IL-2 is given 4 times per week during 27 weeks. After every IL-2 injection, the immune cells number (NK + CTL) augments as it is viewed in Fig. 10a which increases the probability of tumor cell death as it is represented in Fig. 10b. Even if the cure period in this case is longer than the compact tumor case, the tumor

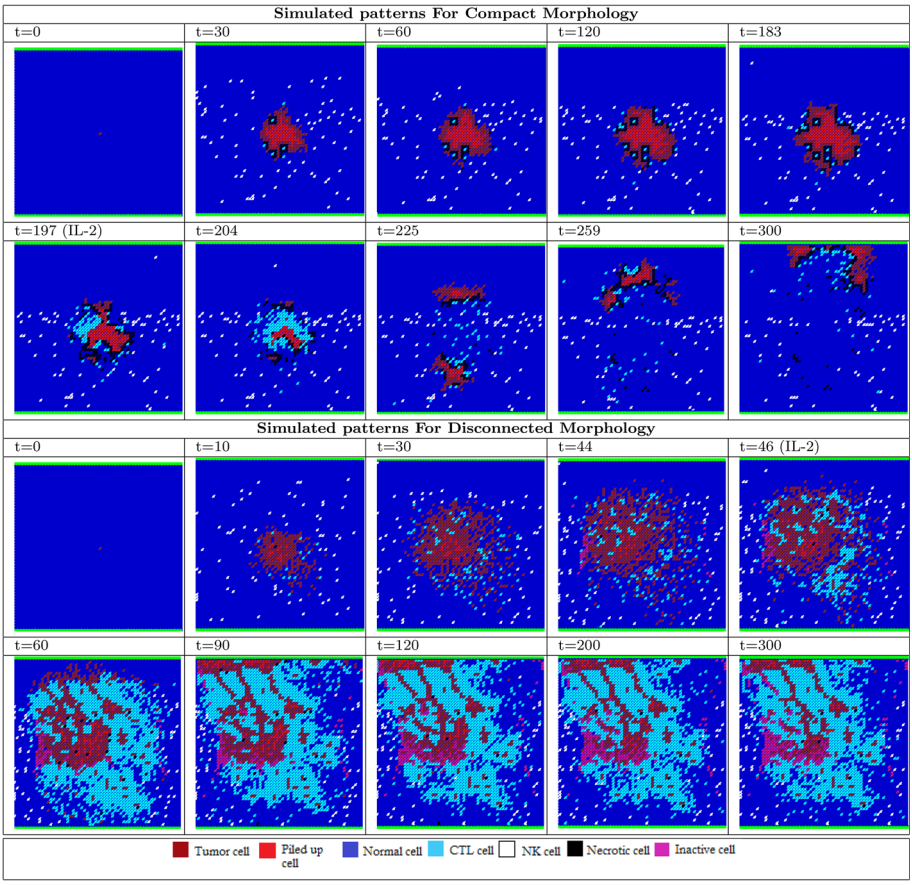


**Fig. 12** Simulated tumor–immune interaction and immunotherapy effect on a $60 \times 60$ square lattice. Parameter values for compact morphology are: $\alpha = 1/L, \lambda_N = 100, \lambda_M = 10, \theta_{div} = 0.3, \theta_{mov} = 10000, \theta_{dth} = 0.01, \theta_{ind} = 9, \theta_{Dctl} = 0.3, \theta_{PL} = 0.5, I_0 = 0.02$. Parameter values for disconnected morphology are: $\alpha = 2/L, \lambda_N = 25, \lambda_M = 10, \theta_{div} = 0.3, \theta_{mov} = 0.1, \theta_{dth} = 0.01, \theta_{ind} = 9, \theta_{Dctl} = 0.3, \theta_{PL} = 0.5, I_0 = 0.02$

mass decreases with unstable oscillations but still in high number. This can be explained by the high probability of tumor cell migration during time. It is noticed that the number of times that the probability of tumor cell division is carried out is low as it is shown in Fig. 10b, whereas the cancerous cells keep moving and keep looking for the adequate area for cell division, which raises the chance of having metastases.

Since the high probability that the cell migration action is carried out, tumor cells keep moving around the tissue and divide everywhere even if near to the capillary vessels in the low response of immune cells, which leads to a disconnected morphology. Immunotherapy starts once the tumor size reaches 7 mm, it is noticed that the CTL cells number for disconnected tumor morphology is higher than the compact morphology case. This may be explained by the dispersed nature of tumor cells which increases the chance of contact between tumor and NK/ or CTL cells, and consequently the recruitment of CTL cells as well as their proliferation due to IL-2 effect augment. Some tumor cells become inactive when they are surrounded by immune cells and cannot migrate nor divide.

The immunotherapy for disconnected tumor was not effective in tumor eradication nor in tumor mass reduction, the cancerous cells still present in large number. Several snapshots of simulated tumor–immune–therapy interactions and their progression are represented in Fig. 12. The same results are obtained when the immunotherapy starts for tumors reaching 300, 500 or 900 mm as it is viewed in Fig. 11.

We have shown that the nutrient consumption not only affects tumor morphology, but also the effectiveness of immunotherapy. As long as there is competition for nutrients between tumor and normal/ or immune cells, the tumor tends to have disconnected morphology with high tumor cell migration, which augments the chance to escape the primary tumor via the blood vessel (metastasis) and set up secondary tumors. In this case, immunotherapy intervention was ineffective. In contrast, when there is low competition for nutrients, tumor cells are very close to each other due to the low cell migration, which leads to a compact morphology. The immunotherapy in this case was remarkably efficient in reducing tumor cell number.

## Conclusion

We have employed a hybrid cellular automata model to describe the immunotherapy effect on tumor–immune interaction. The model includes the tumor growth process in the presence of the innate and specific immune response.

Without immunotherapy intervention, various results depending on the CTL recruitment parameter were found similar to [32] results. On one hand and for high CTL induction, which corresponds to the low value of the CTL recruitment parameter, the immune system was able to reduce the tumor mass due to the high number of CTL. On the other hand, for low CTL induction, which corresponds to the high value of the CTL recruitment parameter, tumor cells grow and invade the local tissue. Tumor morphology generated depends on tumor cell migration process, when the cell motility is low, tumor morphology tends to be compact, whereas, the tumor morphology is disconnected and the cancerous cells are dispersed on the tissue for high cell migration.

What was not mentioned in [32] work is the characterization of tumor morphology, which leads us to discuss some factors of characterization such as the fractality of the boundary and the number of cells on the tumor periphery as well as their biological implication, and to compare the simulated results with the results and observations of other researchers, which showed a good agreement. In addition, In [32] work, the tumor growth stage (avascular, vascular, or metastatic) was not taken into account, and even if tumor size reaches in some cases thousands of cancerous cells, tumor still feeds through the capillary vessels. In our work we have considered that the tumor size once reaches few millimeters, he moves from avascular phase to the development of his own blood vessel phase (angiogenesis), and a third capillary vessel will provide him with nutrients.

Introducing the immunotherapy to the model as a PDE for IL-2 diffusion, leads to different findings depending on tumor morphology and cell motility. For compact tumor, the probability of tumor cell migration was low and the cells on the tumor periphery were in few numbers, which keep the tumor cell away from the capillary vessels. Once injected, the IL 2 stimulates the CTL proliferation as well as the NK cell cytotoxicity, which decreases the number of tumor cells. The immunotherapy in this case was efficient to kill cancer and reduce tumor cells number. For disconnected tumor, the simulations exhibit that the probability of tumor cell migration was high and the cancerous cells tend to keep moving around

the tissue and near to the capillary vessels. The stimulated immune cells intervene in high number, however the continuous movement of tumor makes their mission hard. In this case, immunotherapy was not potent to kill tumor. The cell migration process in the simulated tumor growth has shown a direct influence on the immunotherapy effectiveness.

In summary, we have included the immunotherapy intervention in a hybrid CA-PDE model of tumor growth and immune interaction. In addition, we have studied many characteristics of the simulated growth patterns such as the fractal dimension and number of cells on tumor periphery, which were consistent with the results of other researchers. Tumor morphology, which is related to the cell migration may play a major role in the efficiency of immunotherapy.

## References


1. Agur, Z., Arakelyan, L., Daugulis, P., Ginosar, Y.: Hopf point analysis for angiogenesis models. Discrete Contin. Dyn. Syst. Ser. B **4**, 29–38 (2004)
2. Alarcon, T., Byrne, H., Maini, P.: A cellular automaton model for tumour growth in a heterogeneous environment. J. Theor. Biol **225**, 257–74 (2003)
3. Boissonnas, A., Fetler, L., Amigorena, S.: La stratégie des lymphocytes T cytotoxiques dans l'élimination d'une tumeur solide. MS **23**, 570–572 (2007)
4. Boondirek, A., Lenbury, Y., Wong-ekkabut, J., Triampo, W., Tang, I., Picha, P.: A stochastic model of cancer growth with immune response. J. Korean Phys. Soc. **49**, 1652–1666 (2006)
5. Bru, A., Albertos, S., Subiza, J., Garcia-Asenjo, J.: The universal dynamics of tumor growth. Biophys. J. **85**, 2948–61 (2003)
6. Cabrera, L., Galvez, J., Lajarin, F., Rubio, G., Aparicio, P., Garcia-Penarrubia, P.: Conjugation between cloned human NK cells (H7.8) and K562/MOLT4 tumor cell systems: saturability, binding parameters, and population distribution of conjugates. Cell Immunol. **169**, 133–141 (1996)
7. Chaplain, M.: Avascular growth, angiogenesis and vascular growth in solid tumours: the mathematical modeling of the stages of tumor development. Math. Comput. Model **23**, 47–87 (1996)
8. Cho, D., Campana, D.: Expansion and activation of natural killer cells for cancer immunotherapy. Korean J. Lab. Med. **29**, 89–96 (2009)
9. M. Clinical reference, Interleukin-2, Medscape Drugs Dis
10. Costello, R., Gastaut, J., Olive, D.: Tumor escape from immune surveillance. Arch. Immunol. Ther. Exp. (Warsz) **47**, 83–88 (1999)
11. Cross, S.: Fractals in pathology. J. Pathol. **182**, 1–8 (1997)
12. De Pillis, L., Gu, W., Radunskaya, A.: Mixed immunotherapy and chemotherapy of tumors: modeling, applications and biological interpretations. J. Theor. Biol. **238**, 841–862 (2006)
13. Delves, P., Roitt, I.: The immune system first of two parts. N. Engl. J. Med. **343**, 37–49 (2000)
14. Dunn, S.: Understanding cancer drug dosing. CancerGuide (2000). http://www.cancerguide.org/drugdosing.html
15. Elmouki, I., Saadi, S.: Quadratic and linear controls developing an optimal treatment for the use of BCG immunotherapy in superficial bladder cancer. Optim. Control Appl. Methods **37**, 176–189 (2016)
16. Ferreira, S., Martins, M., Vilela, M.: A growth model for primary cancer. Phys. A **261**, 569–580 (1998)
17. Ferreira, S., Martins, M., Vilela, M.: A reaction diffusion model for the growth of avascular tumor. Phys. Rev. E **65**, 021907–8 (2002)
18. Folkman, J., Klagsbrun, M.: Angiogenic factors. Science **235**, 442–447 (1987)
19. Fyfe, G., Fisher, R., Rosenberg, S., Sznol, M., Parkinson, D., Louie, A.: Results of treatment of 255 patients with metastatic renal cell carcinoma who received high-dose recombinant interleukin-2 therapy. J. Clin. Oncol. **13**, 688–696 (1995)
20. Gibbs, W.: Untangling the roots of cancer. Sci. Am. **18**, 30–39 (2008)
21. Greenspan, H.: On the growth and stability of cell cultures and solid tumors. J. Theor. Biol **56**, 229–242 (1976)
22. Gyllenberg, M., Webb, G.: Quiescence as an explanation of gompertzian tumor growth. Growth Dev. Aging **53**, 25–33 (1989)
23. Jackson, T.: Vascular tumor growth and treatment: consequences of polyclonality, competition, and dynamic vascular support. J. Math. Biol **44**, 201–226 (2002)

24. Jiao, Y., Torquato, S.: Emergent behaviors from a cellular automaton model for invasive tumor growth in heterogeneous microenvironments. PLoS Comput. Biol. **7**, e1002314 (2011)
25. Kirschener, D., Panetta, J.: Modeling immunotherapy of the tumor–immune interaction. J. Math. Biol **37**, 235–252 (1998)
26. Lafreniere, R., Rosenberg, S.: Successful immunotherapy of murine experimental hepatic metastases with lymphokine activated killer cells and recombinant interleukin 2. Cancer Res. **45**, 3735–3741 (1985)
27. Laird, A.K.: Dynamics of tumour growth. Br. J. Cancer **13**, 490–502 (1964)
28. Landini, G., Rippin, J.: Fractal dimensions of the epithelial connective tissue interfaces in premalignant and malignant epithelial lesions of the floor of the mouth. Anal. Quant. Cytol. Histol. **15**, 144–149 (1993)
29. Landini, G., Rippin, J.: How important is tumour shape? Quantification of the epithelial-connective tissue interface in oral lesions using local connected fractal dimension analysis. J. Pathol. **179**, 210–217 (1996)
30. Liao, W., Lin, J., Leonard, W.: Interleukin-2 at the crossroads of effector responses, tolerance, and immunotherapy. Immunity **38**, 13–25 (2013)
31. Lin, A.: A model of tumor and lymphocyte interactions. Discrete Contin. Dyn. Syst **4**, 241–266 (2004)
32. Mallet, D., De Pillis, L.: A cellular automata model of tumor–immune system interactions. J. Theor. Biol **239**, 334–350 (2006)
33. Matzavinos, A., Chaplain, M.: Mathematical modelling of the spatiotemporal response of cytotoxic T lymphocytes to a solid tumour. Math. Med. Biol. **21**, 1–34 (2004)
34. Mazumder, A., Rosenberg, S.: Successful immunotherapy of natural killer resistant established pulumonary melanoma metastases by the intervenous adoptive transfer of syngeneic lymphocytes activated in vitro by interleukin 2. J. Exp. Med. **159**, 495–507 (1984)
35. Moisy F.: Fractal dimension using the 'box-counting' method for 1d, 2d and 3d sets. MATLAB's File Exch. (2006). http://www.mathworks.com/matlabcentral/fileexchange/13063-boxcount/content/boxcount/html/demo.html
36. Monteagudo, A., Santos, J.: A cellular automaton model for tumor growth simulation. Adv. Intell. Soft Comput. **154**, 147–155 (2012)
37. Mule, J., Shu, S., Schwarz, S., Rosenberg, S.: Adoptive immunotherapy of established pulmonary metastases with lak cells and recombinant interleukin-2. Science **225**, 1487–1489 (1984)
38. Naoyo, N., Hirohisa, Y., Takashi, N., Toshiharu, K., Masamichi, K.: Angiogenesis in cancer. Vasc. Health Risk Manag. **2**, 213–219 (2006)
39. Osmanoglu F.: The journey of drugs through the body. Health Med. **92** (2013). http://www.fountainmagazine.com/Issue/detail/the-journey-of-drugs-through-thebody-march-april-2013
40. Phillips, J., Lanier, L.: Dissection of the lymphokine-activated killer phenomenon. relative contribution of peripheral blood natural killer cells and T lymphocytes to cytolysis. J. Exp. Med. **164**, 814–825 (1986)
41. Powathil, G.G., Gordon, K.E., Hill, L.A., Chaplain, M.A.J.: Modelling the effects of cell-cycle heterogeneity on the response of a solid tumour to chemotherapy: biological insights from a hybrid multiscale cellular automaton model. J. Theor. Biol. **308**, 1–19 (2012)
42. Qi, A., Zheng, X., Du, C., An, B.: A cellular automaton model of cancerous growth. J. Theor. Biol **161**, 1–12 (1993)
43. Rabinowich, H., Banks, M., Reichert, T., Logan, T., Kirkwood, J., Whiteside, T.: Expression and activity of signaling molecules n t lymphocytes obtained from patients with metastatic melanoma before and after interleukin 2 therapy. Clin. Cancer Res. **2**, 1263–1274 (1996)
44. Riedel, H.: Models for tumour growth and differentiations. In: The Cancer Handbook. Wiley (2007)
45. Roose, T., Chapman, S.J., Maini, P.K.: Mathematical models of avascular tumor growth. SIAM Rev. **49**, 179–208 (2007)
46. Rosenberg, S., Lotze, M.: Cancer immunotherapy using interleukin-2 and interleukin-2-activated lymphocytes. Annu. Rev. Immunol. **9**, 681–709 (1986)
47. Rosenberg, S., Lotze, M., Muul, L., Chang, A., Avis, F., Leitman, S., Linehan, W., Robertson, C., Lee, R., Rubin, J., et al.: A progress report on the treatment of 157 patients with advanced cancer using lymphokine-activated killer cells and interleukin-2 or high-dose interleukin-2 alone. N. Engl. J. Med. **316**, 889–897 (1987)
48. Rosenberg, S., Lotze, M., Yang, J., et al.: Experience with the use of high dose interleukin-2 in the treatment of 652 cancer patients. Ann. surg. **210**, 474–485 (1989)
49. Rosenberg, S., Yang, J., Topalian, S., Schwartzentruber, D., Weber, J., Parkinson, D., Seipp, C., Einhorn, J., White, D.: Treatment of 283 consecutive patients with metastatic melanoma or renal cell cancer using highdose bolus interleukin 2. JAMA **271**, 907–913 (1994)
50. Schwartzentruber, D.: In vitro predictors of clinical response in patients receiving interleukin-2-based immunotherapy. Curr. Opin. Oncol. **5**, 1055–1058 (1993)

51. Smith, F., Downey, S., Klapper, J., Yang, J., Sherry, R., Royal, R., Kammula, U., Hughes, M., Restifo, N., Levy, C., White, D., Steinberg, S., Rosenberg, S.: Treatment of metastatic melanoma using interleukin-2 alone or in conjunction with vaccines. Clin. Cancer Res. **14**, 5610–5618 (2008)
52. Smolle, J., Stettner, H.: Computer simulation of tumour cell invasion by a stochastic growth model. J. Theor. Biol. **160**, 63–72 (1993)
53. Trinchieri, G., Matsumoto-Kobayashi, M., Clark, S., Seehra, J., London, L., Perussia, B.: Response of resting human peripheral blood natural killer cells to interleukin 2. J. Exp. Med. **160**, 1147–1169 (1984)
54. West, W., Tauer, K., Yanelli, J., et al.: Constant-infusion recombinant inetleukin-2 in adoptive immunotherapy of advanced cancer. N. EngL. J. Med. **316**, 898–905 (1987)
55. Yang, J., Sherry, R., Steinberg, S., Topalian, S., Schwartzentruber, D., Hwu, P., Seipp, C., Rogers-Freezer, L., Morton, K., White, D., Liewehr, D., Merino, M., Rosenberg, S.: Randomized study of high-dose and lowdose interleukin-2 in patients with metastatic renal cancer. J. Clin. Oncol. **21**, 3127–3132 (2003)
56. Zouhri, S., Saadi, S., Rachik, M.: Simulating the tumor growth with cellular automata models. IJCA **108**, 5–11 (2014)